

## 5.4: Coupled Models and Climate Projections

Peter R. Gent

National Center for Atmospheric Research,  
Boulder, Colorado, USA.

[gent@ucar.edu](mailto:gent@ucar.edu)

### 5.4.1. Formulation of Coupled Models

Coupled climate models consist of atmosphere, land and sea ice components, as well as the ocean component. The atmosphere component is similar to the ocean in that it solves the primitive equations of motion, usually with hydrostatic balance, the continuity equation and predictive equations for temperature and specific humidity. The vertical coordinate is usually pressure, or terrain-following, or a combination of both. A comprehensive review of atmosphere components can be found in Randall et al. (2007). The land surface component usually solves equations in the vertical direction for heat and water that include many complex interactions at the land surface and soil layers below. It also calculates water runoff, which is then routed by a realistic horizontal pattern of river basins to create the river runoff field that is sent to the ocean component. The sea ice component solves a complicated equation for the ice rheology and thermodynamic equations for the heat balance of the sea ice. When the ice melts, fresh water is sent to the ocean component, and the ocean receives a brine rejection flux when the sea ice is formed.

The formulation of the ocean component of coupled models has been described in detail earlier in Chapter 5.1. In that chapter it is conjectured, and I concur, that ocean model simulations depend much more strongly on the parameterizations of mixing and the effects of unresolved scales than on details of the numerical discretization of the equations (Chassignet et al., 1996). The parameterization of vertical mixing has been discussed earlier in Chapter 3.3, and the parameterization of unresolved lateral transport in Chapter 3.4.

The first climate model that used realistic geometry was assembled by Syukuro Manabe, Kirk Bryan and co-workers at the Geophysical Fluid Dynamics Laboratory (GFDL), and the results were published in two landmark papers; Manabe et al. (1975) and Bryan et al. (1975). The horizontal grid spacing was  $5^\circ \times 5^\circ$ , and there were nine vertical levels in the atmosphere component and five levels in the ocean component. Since then, the components have become much more sophisticated and complex, and the horizontal resolution has increased to about  $1^\circ \times 1^\circ$  or finer in present day climate models that use about 30-60 vertical levels in the atmosphere and ocean components.

### 5.4.2. Flux Adjustments

Through most of the 1990s, present day control runs of all climate models would quite quickly drift away from the realistic initial conditions with which they were initialized. This drift was usually corrected by the use of flux adjustments described in Sausen et al. (1988), which could be calculated in two different ways. The heat and fresh water fluxes between the atmosphere and ocean components were diagnosed when the atmosphere component was run using observed sea surface temperatures (SSTs) and the ocean component was run using observed wind stresses and atmosphere surface variables. These flux diagnoses were quite different, and their differences were the flux adjustments. Alternatively, the coupled model was run with strong relaxation back to observations of SST and sea surface salinity, and these relaxation terms were used as the flux adjustments. The flux adjustments were added to the heat and fresh water fluxes between the atmosphere and ocean in a present day coupled control run at each time step. This method corrected most of the model drift, but was very unsatisfactory because flux adjustments are completely unphysical, mask deficiencies in the atmosphere and ocean components that require their use, and likely give an unrealistic response to large perturbations of the climate system.

44 The first model that could maintain the present day temperature climate in a control run without the use of flux  
45 adjustments was the Community Climate System Model, version 1 (CCSM1). A 300 year control simulation that  
46 showed very little drift in surface temperature was run during the second half of 1996, and documented in Boville &  
47 Gent (1998). The reason for this success was refinements of the atmosphere, and especially the ocean component, so  
48 that the surface heat flux produced by the two components in stand-alone runs was close enough to be compatible.  
49 However, the ocean salinity did drift because CCSM1 did not have a realistic river runoff component. A history of  
50 this success is contained in a recent review by Gent (2011). Quite quickly, the climate centers in Australia and the  
51 United Kingdom implemented two of the new ocean parameterizations from the CCSM1, and were also able to run  
52 their models with much reduced, or without, flux adjustments (Hirst et al., 1996, Gordon et al., 2000).

53 Now, almost all climate models are run without using flux adjustments. A consequence is that current climate  
54 models cannot reproduce the present day atmosphere surface temperature and SSTs quite as well as when flux  
55 adjustments were used. However, this small detraction is far outweighed by the fact that climate models no longer  
56 use the unphysical flux adjustments. For example, in some models the flux adjustment transported nearly as much  
57 heat northwards in the North Atlantic Ocean as did the ocean component. This can be seen in Figure 2.3.1 of  
58 northward heat transport in the Hadley Centre models with and without flux adjustments shown in Section 2.3.3 of  
59 the first edition of this book by Wood & Bryan (2001).

#### 60 5.4.3. Control Runs

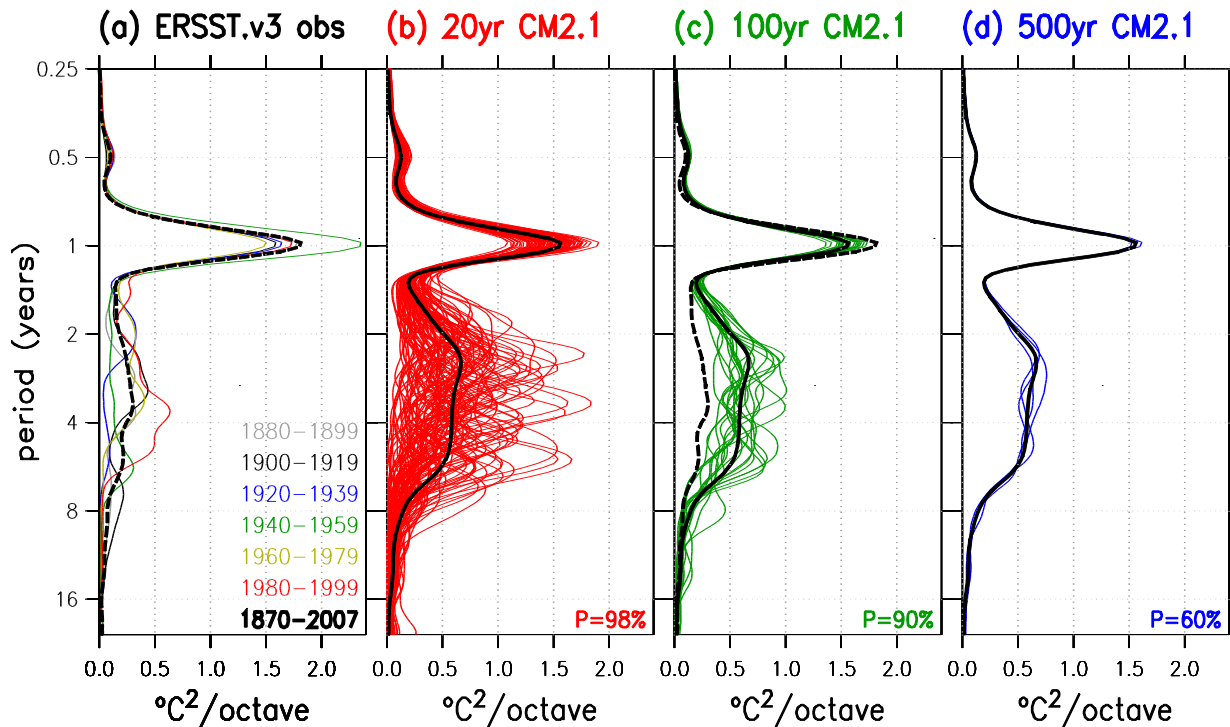
61 A control run is an integration of a climate model in which the solar input at the top of the atmosphere component  
62 has a repeating annual cycle, and all the other forcings have a repeating annual cycle or are kept constant in time.  
63 The forcings can include the atmospheric concentrations of carbon dioxide (CO<sub>2</sub>) and other greenhouse gases, and  
64 the distributions of several aerosols that affect the atmosphere radiation balance. Quite often a control run is made  
65 using forcings from present day conditions. This has the advantage that the simulation can be compared to a whole  
66 range of observations that have been made in the recent past. However, it is well known that the present-day climate  
67 is not in equilibrium because important forcings, namely the greenhouse gas concentrations and aerosol emissions,  
68 have been increasing quite rapidly. Therefore, an alternative control run is made for 'pre-industrial' conditions,  
69 when it is assumed that the climate was in equilibrium. Pre-industrial is often chosen to be 1850, which is not truly  
70 before the industrial revolution. However, 1850 is chosen as a compromise between only a very small increase in  
71 CO<sub>2</sub> over truly pre-industrial levels, and reducing the length of climate model runs between pre-industrial times and  
72 the present day.

73 Choosing the initial conditions to start an 1850 control run is not straightforward because the ocean, sea ice and  
74 land states for this period are unknown. The atmosphere initial condition is not as important because it is forgotten  
75 within a few weeks of the start of the run, so a state from an atmosphere model run forced by observed SSTs is  
76 usually chosen. Present day states for the sea ice are usually chosen, although the 1850 sea ice volume is thought to  
77 be larger, so that sea ice should grow during the control run. It is important not to put far too much sea ice into the  
78 initial condition, because when it melts quickly, it will suppress convection in the ocean component which can take  
79 a few hundred years to overcome. It is also important that the water content of the soil in the land component is  
80 initialized realistically, because the timescale to change the water content of the deepest soil level can also be a few  
81 hundred years. The traditional way to initialize the ocean component is to use a climatology from the late 20<sup>th</sup>  
82 century; Levitus et al. (1998) and Steele et al. (2001). This initial condition has a larger heat content than in 1850,  
83 so that the climate model would be expected to lose heat initially from the ocean component and the whole system,  
84 although this does not happen in all climate models as some have the ocean gaining heat in 1850 control runs (e.g.  
85 Griffies et al. 2011).

86 The SST acts as a negative feedback on the atmosphere-to-ocean heat flux, so it would be expected that the  
87 atmosphere-to-ocean heat flux, and consequently the top of atmosphere heat budget, would converge towards zero  
88 after a few decades of an 1850 control run. However, in practice this seldom happens because the ocean heat loss or  
89 gain occurs in the deeper ocean and not in the surface layers. The climate model heat loss or gain is often almost  
90 constant in time and is difficult to get very close to zero. Most climate modeling groups aim to get the globally-

91 averaged heat imbalance less than  $0.1 \text{ W/m}^2$ , usually by tuning a cloud parameter or two in the atmosphere  
 92 component (e.g. Gent et al. 2011). Even so, this rate of ocean heat loss or gain sustained over an integration of 1000  
 93 years means the ocean volume average temperature decreases or increases by  $0.2^\circ\text{C}$  compared to the  $3.7^\circ\text{C}$  value in  
 94 the Levitus et al. (1998) data used to initialize ocean components. Many well constructed climate models conserve  
 95 water quite well, even though not to machine accuracy. The volume average ocean salinity can vary because of  
 96 changes in the volume of sea ice and soil water content over the course of the integration. However, the volume  
 97 average ocean salinity changes only marginally even over a 1000 year control run if water is almost conserved.

98 One disadvantage of a pre-industrial control run compared to a present-day control run is that there are very few  
 99 observations relevant to that period. However, an 1850 control run does reveal the internal variability of the climate  
 100 model given repeating annual cycle forcing, which is important to document. Variability occurs on all timescales  
 101 from the diurnal to centennial, and this variability can be compared to late 20<sup>th</sup> century observations. For example,  
 102 the largest interannual signal in the climate system is the El Nino/Southern Oscillation (ENSO) phenomena. This  
 103 has been a difficult signal for climate models to simulate well. However, there has been significant progress in  
 104 recent years. For example, Wittenberg (2009) looks at ENSO in a 2000 year control run of the GFDL CM2.1  
 105 climate model, and shows there is decadal and centennial variability in both the frequency and amplitude of the  
 106 signal. Figure 1 shows the frequency of NINO3 area ( $90^\circ\text{W}$ - $150^\circ\text{W}$ ,  $5^\circ\text{S}$ - $5^\circ\text{N}$ ) monthly SST anomalies from  
 107 observations and the CM2.1 when the run is divided into 20, 100, and 500 year segments. The amplitude has a lot of  
 108 variability over the 20 year segments, and still significant variability over the 100 year segments of the control run.  
 109 A period in the run can be found where the model ENSO matches quite well the observed record from 1956 to 2010.  
 110 The ENSO signal in the recently completed CCSM4 model is significantly improved over earlier model versions  
 111



112  
 113 Figure 1. Power spectra of NINO3 SSTs as a function of the period in octaves of the annual cycle. (a) Spectra for six 20 year  
 114 epochs (solid) and one 138 year epoch (dashed and repeated in (c)) from the ERSST observations, and spectra from the CM2.1  
 115 pre-industrial control run for (b) 20 year epochs, (c) 100 year epochs and (d) 500 year epochs, where the thick black solid line is  
 116 the spectrum from the full 2000 year run. From Wittenberg (2009).

117 (Neale et al., 2008), and the above comments also apply to ENSO in the 1300 year long CCSM4 1850 control run  
118 (Deser et al., 2012). The other purpose of an 1850 control run is to provide initial conditions for an ensemble of  
119 integrations of the model from 1850 to the present day, which are often called 20<sup>th</sup> century runs.

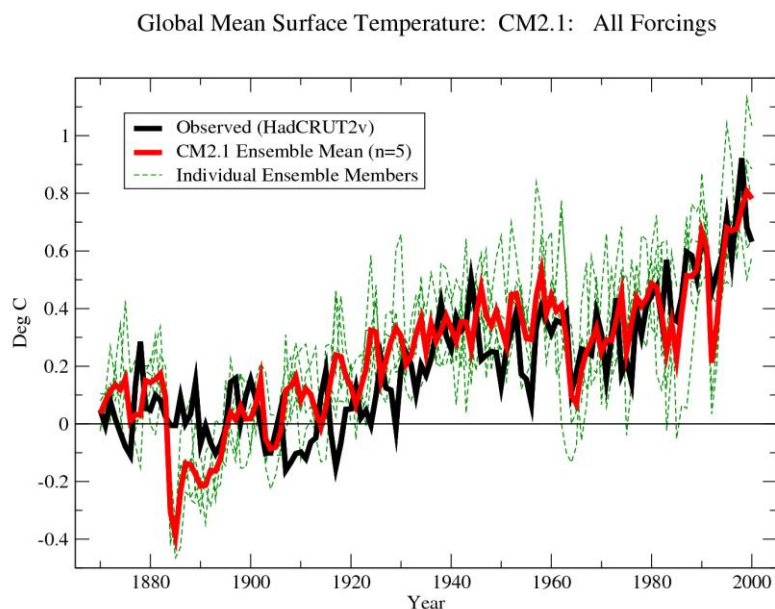
120

#### 121 5.4.4. 20<sup>th</sup> Century Runs

122 Time series over 1850 to the present day of four or five types of input variables are needed to force 20<sup>th</sup> century  
123 runs. They are the atmospheric concentrations of CO<sub>2</sub> and other greenhouse gases, the level of solar output, the  
124 levels of natural and human-made aerosols, the amount of atmospheric aerosols from volcanic eruptions, and some  
125 models use historical changes in land use in the land component. The volcanic aerosol level is determined from the  
126 observed levels of aerosols from recent eruptions, such as El Chicon in 1982 and Pinatubo in 1991, and then scaled  
127 by the size of eruptions earlier in the period, such as the large Krakatoa eruption in 1883. Usually, an ensemble of  
128 these 20<sup>th</sup> century runs is made with each climate model, where the initial conditions are taken from different times  
129 in the 1850 control run. These initial conditions are chosen after a few hundred years of the control run, so that the  
130 modeled climate system, including the upper kilometer or so of the ocean, has had time to come into equilibrium. If  
131 a climate model is to be useful, then its 20<sup>th</sup> century runs must reproduce well many of the observed changes in the  
132 earth's climate over the last 150 years. Most of these comparisons with observations will use the last 50 years of  
133 these runs, which is when virtually all of the observations were made.

134 The best measured quantities going back to 1850 are surface temperature over land and SST. These can be  
135 combined into a globally-averaged surface temperature with only a small uncertainty, so that it is well known that  
136 the earth's surface temperature has increased by about 0.7°C over the time 1850 to 2000. Figure 2 shows both the  
137 observations and the ensemble of five 20<sup>th</sup> century simulations using the GFDL CM2.1 model. The CM2.1 ensemble  
138 mean reproduces the observations rather well. There are an enormous number of other quantities that can be

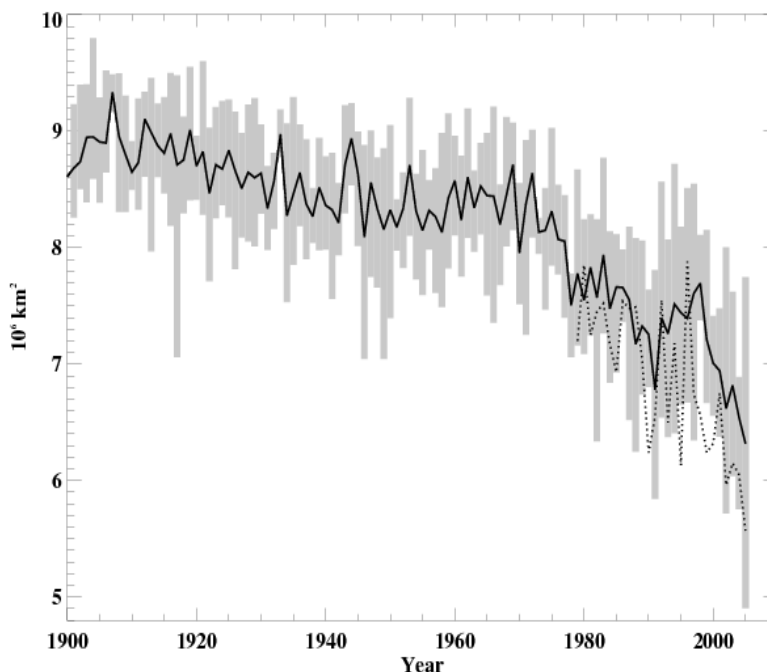
139



140

141 Figure 2. Globally-averaged surface air temperature over 1870 to 2000 from the HadCRUT2v observations and both the  
142 individual members and the ensemble mean from 20<sup>th</sup> century runs using the GFDL CM2.1 model. From Knutson et al. (2006).

143 compared to observations, and choices have to be made about which are compared because they are most important.  
144 For example, satellite observations of Arctic sea ice between 1979 and 2012 have shown a very significant decrease  
145 in the ice area during September, which is the month when the ice area is a minimum. If the climate model is to be  
146 used to project the future state of Arctic sea ice, including when the Arctic Ocean might be virtually ice free in  
147 September, then the model must reproduce the observations well within the ensemble of 20<sup>th</sup> century runs. Figure 3  
148 shows the September Arctic sea ice area from satellite observations (dotted line), and the ensemble mean and spread  
149 of 20<sup>th</sup> century runs using the CCSM version 4 (solid line and shading) through 2005, which is when the 20<sup>th</sup> century  
150 runs end. The CCSM4 reproduces the observed decline of September sea ice quite well.  
151

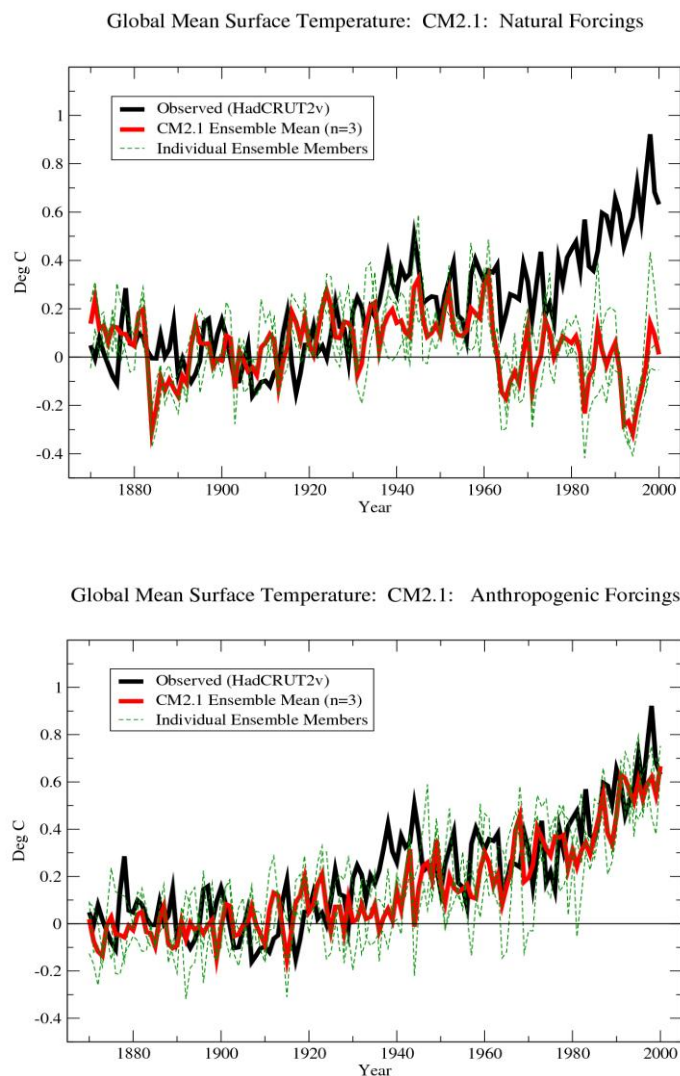


152 Figure 3. Area of Arctic sea ice in September from satellite observations (dotted line) and the ensemble mean (solid line) and  
153 spread (gray shading) from six 20<sup>th</sup> century runs using the CCSM4. From Gent et al. (2011).

154 Another use of 20<sup>th</sup> century runs is to determine the cause of the earth's warming that has increased markedly  
155 since the mid 1970s. Additional runs are made where all the natural forcings are retained and the levels of the  
156 greenhouse gases and man-made aerosols are kept at their pre-industrial values, and the converse of this run where  
157 just the anthropogenic forcings are allowed to vary. Figure 4 shows the globally-averaged surface temperature from  
158 ensembles of these two runs using the GFDL CM2.1 model. The conclusion is that the all natural forcings runs  
159 cannot explain the accelerated warming since 1975, whereas the anthropogenic forcings runs explain the observed  
160 temperature rise within the internal variability of the model. The confidence with which this result can be stated  
161 depends on the amplitude of the model internal variability and the length of time since the model surface  
162 temperature started to increase markedly. The increase in the model surface temperature over the last 35 years is  
163 now above two standard deviations of most models' internal variability. The 4<sup>th</sup> Assessment Report of the  
164 Intergovernmental Panel on Climate Change (IPCC), (Solomon et al., 2007), concluded that it is now 'very likely'  
165 that the recent warming is due to anthropogenic causes. The level of certainty about this conclusion has increased in  
166 successive IPCC reports as, over time, the size of the observed temperature increase has become considerably larger  
167 compared to climate models' internal variability. It is important to note here that there is considerable uncertainty  
168 about the parameterization of clouds and the interaction of aerosols and clouds in the atmosphere component of  
169 climate models. A detailed discussion of these topics can be found in Chapters 1 and 2 of Solomon et al. (2007).

170 5.4.5 Future Projections

171 In order for a climate model to run projections, the future levels need to be estimated of the same four or five  
172 types of input variables that were required for 20<sup>th</sup> century runs. The future level of solar output is usually chosen to  
173 be constant, although a very small 11 year cycle is sometimes imposed. Future volcanic eruptions are unknown, so  
174 a constant background level of volcanic aerosols is usually used. The future levels of natural aerosols are often  
175 chosen to be constant, along with a gradual reduction of man-made aerosols later in the 21<sup>st</sup> century. Finally, a  
176 scenario for the future atmosphere concentrations of CO<sub>2</sub> and other greenhouse gases has to be chosen. There is  
177 much debate and uncertainty about whether future emissions of CO<sub>2</sub> will remain at their present levels, accelerate  
178 over the next few decades, or reduce in the second half of the 21<sup>st</sup> century as the world turns to alternate energy  
179 sources. Because of this uncertainty, climate models have been run with a wide variety of scenarios for the future



180  
181 Figure 4. Globally-averaged surface temperature 1870-2000 from observations, and ensembles of (a) all natural forcing runs, and  
182 (b) anthropogenic forcings runs using the GFDL CM2.1. From Knutson et al. (2006).

183 concentrations of CO<sub>2</sub>. These concentrations are usually based on a fixed percentage of the CO<sub>2</sub> emissions  
184 remaining in the atmosphere, or are the output of integrated assessment models which use CO<sub>2</sub> emissions as input.  
185 This approach ignores the possible feedbacks from the land and ocean components, which may take up less or more  
186 of the emitted CO<sub>2</sub> in the future compared to the past. If a climate model is to predict the future CO<sub>2</sub> concentrations  
187 given the emissions, then it must have an interactive carbon cycle that can predict the future levels of CO<sub>2</sub> uptake by  
188 the land and ocean components (see Chapter 6.4).

189 An informative future projection is obtained if the concentrations of CO<sub>2</sub> and other greenhouse gases are kept  
190 constant at their present day values. This is called a ‘commitment’ run, because it shows the future changes that we  
191 have committed to by raising the atmosphere CO<sub>2</sub> concentration to its present level. Assuming no future changes in  
192 the forcings, most climate models simulate an increase in the globally-averaged surface temperature of between 0.2°  
193 and 0.4°C over the next 100 years, see Figure 5b. This increase depends on the model’s equilibrium climate  
194 sensitivity, sensitivity to aerosols, and the rate of ocean heat uptake. The equilibrium climate sensitivity is defined as  
195 the surface temperature increase due to a doubling of the CO<sub>2</sub> concentration when the ocean component is a simple  
196 mixed layer model. Using a mixed layer model ensures an equilibrium response after about 30 years, rather than the  
197 order 3000 years if the full depth ocean component is used, (Stouffer 2004, Danabasoglu and Gent 2009). It is  
198 interesting to note that the future temperature rise is very small after about 50 years of a commitment run. This is in  
199 sharp contrast to the future heat uptake by the ocean component and the resulting sea level rise due to thermal  
200 expansion, which increase almost linearly with time over the entire duration of commitment runs, see Figure 5c. As  
201 stated above, the time for the full ocean to reach equilibrium is on the order of 3000 years, so that the ocean heat  
202 content will not start to asymptote away from the linear increase for well over 1000 years. A similar, extremely long  
203 timescale is also relevant for glaciers and ice caps to come into equilibrium with the temperature increase that we  
204 have committed to. The conclusion is that, even if future temperature rises are stabilized by reductions in CO<sub>2</sub>  
205 emissions, the sea level rise we have committed to will continue for the next 1000 years. This extremely long  
206 timescale for sea level rise is frequently not appreciated; more discussion is in Chapter 6.1.

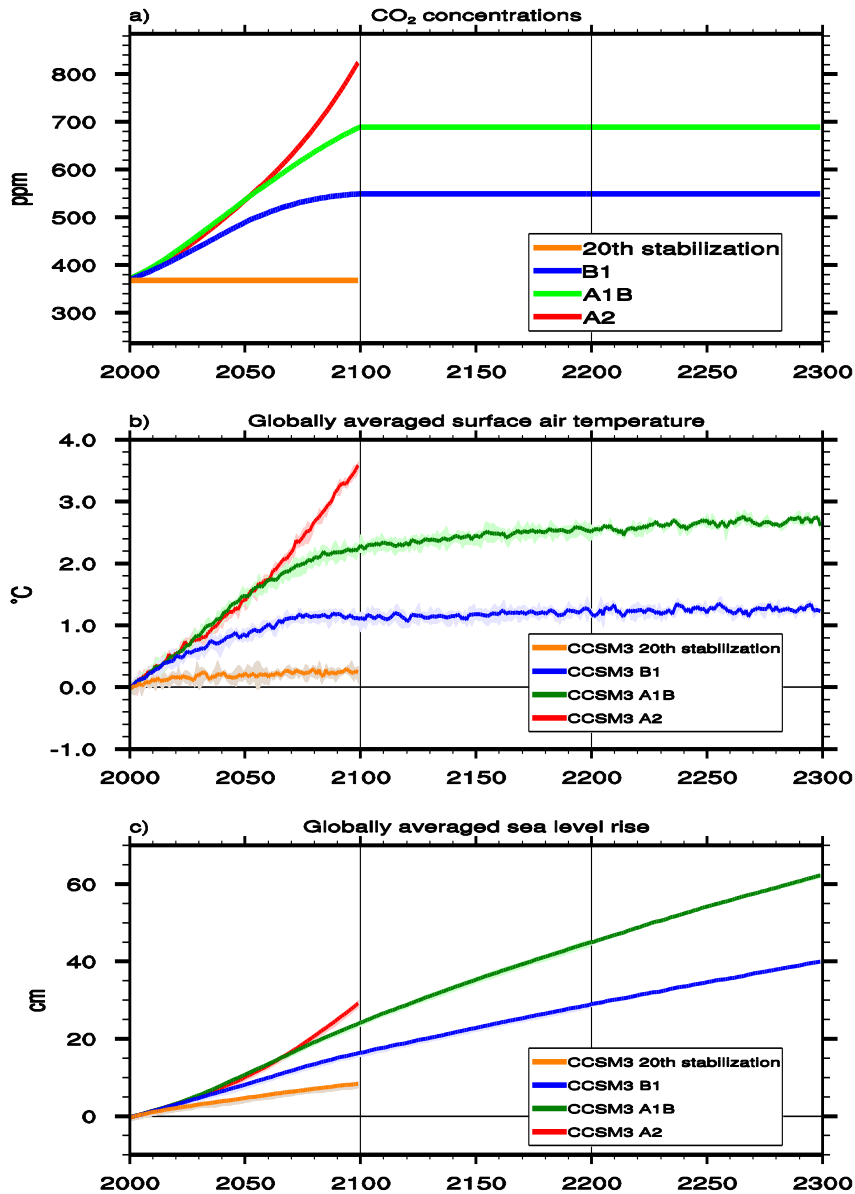
207 Figure 5a shows the future CO<sub>2</sub> concentrations from three different scenarios and Figure 5b shows the resulting  
208 globally-averaged surface temperatures. As is to be expected, the faster the rise in greenhouse gases, the faster the  
209 rise in surface temperature. The rate of temperature increase varies across climate models depending upon their  
210 equilibrium climate sensitivity, sensitivity to aerosols, on the rate of heat uptake by their ocean components, and  
211 several other factors. Some future projections have been run where the CO<sub>2</sub> concentration reaches a maximum and  
212 is then kept constant. The temperature increases quickly, but then only increases slowly when CO<sub>2</sub> is constant, and  
213 so do other important quantities such as the rate of decrease of Arctic sea ice. However, as shown in Figure 5c,  
214 ocean heat uptake, and the resulting rise in sea level due to thermal expansion, do not level off; the rate of heat  
215 uptake only decreases slightly once the CO<sub>2</sub> concentrations are kept constant because of the very long ocean  
216 adjustment timescale.

217

#### 218 *5.4.6 North Atlantic Meridional Overturning Circulation*

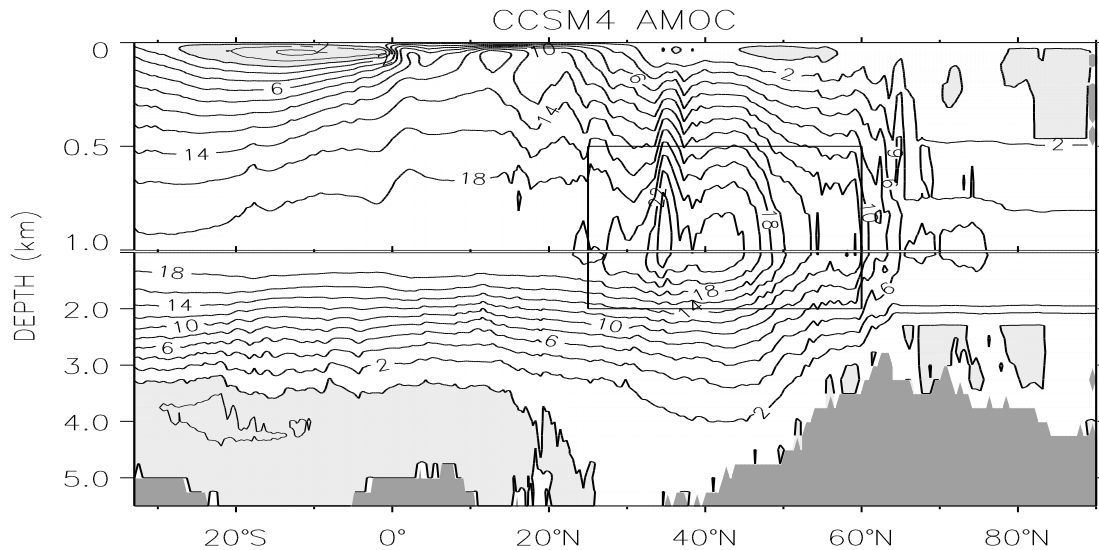
219

220 The Gulf Stream transports warm water northwards in the North Atlantic. Most of this water returns to the south  
221 in the gyre circulation in the upper ocean, but some is returned southwards in a vertical circulation. Deep water is  
222 formed in the Labrador and Greenland/Iceland/Norwegian Seas and is then returned south in the deep western  
223 boundary current along the west side of the North Atlantic. This meridional overturning circulation (MOC) is  
224 important because it carries a majority of the heat that is transported towards the Arctic by all the oceans in the  
225 Northern Hemisphere. This heat transport modulates the climate of Western Europe compared to other land masses  
226 at the same latitude. An equivalent, large-scale vertical overturning circulation does not occur in the North Pacific  
227 Ocean. An important question is how future increases in CO<sub>2</sub> will affect modes of climate variability, such as the  
228 North Atlantic MOC?



229  
 230  
 231 Figure 5. a) CO<sub>2</sub> concentrations from four future scenarios, b) the resulting globally-averaged surface temperature increase,  
 232 and c) the globally-averaged sea level rise due to thermal expansion from runs using the CCSM3. From Meehl et al. (2006).  
 233

234 In models, the MOC is characterized by the streamfunction formed by the meridional and vertical velocities when  
 235 the continuity equation is integrated zonally across the ocean basins. A typical Atlantic Ocean MOC streamfunction  
 236 from the CCSM4 is shown in Figure 6. It shows water moving northwards in the upper kilometer, sinking down to  
 237 between 2 and 4 km between 60° and 65°N, and then returning southwards. Note that a large fraction of this return  
 238 flow crosses the equator into the Southern Hemisphere. Below this deep return flow, the negative contours show a  
 239 weak northward flow near the ocean floor, which is the model representation of Antarctic Bottom Water flowing  
 240 northwards. The magnitude of the North Atlantic MOC is virtually always taken to be the maximum value of the  
 241 overturning streamfunction in Sverdrups (Sv), which is usually at a depth of about 1km. Note that this maximum  
 242 value cannot be directly measured from observations, although estimates can be made both from observations at  
 243 particular latitudes (Cunningham et al., 2007) and using assimilation models of ocean circulation (Wunsch &  
 244 Heimbach, 2006).



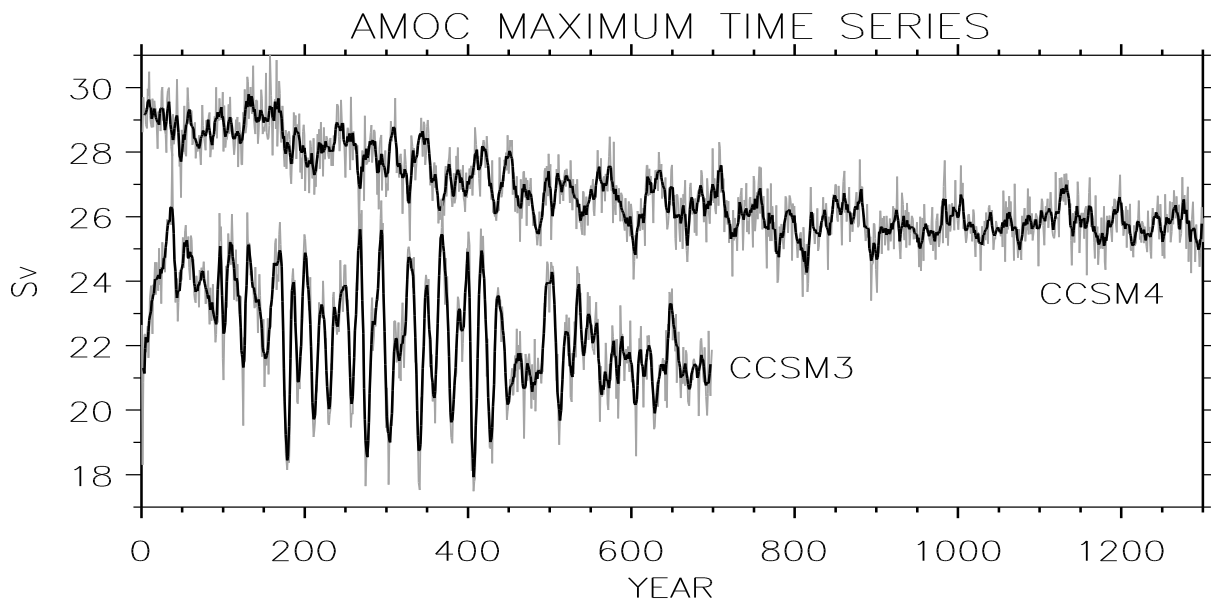
245

Figure 6 North Atlantic meridional overturning streamfunction in Sv from the CCSM4. From Danabasoglu et al. (2012).

246

Figure 7 shows the maximum North Atlantic MOC values from the pre-industrial control runs of the climate models CCSM3 and CCSM4 (from the box shown on Figure 6). It shows that the maximum value takes on the order of 400-500 years to adjust to the model climatology from the initial condition. This is one reason why the initial conditions for 20<sup>th</sup> century runs described earlier should be taken after 500 years or longer of the control runs. Figure 7 also shows a large difference in the internal variability of the North Atlantic MOC between the two versions of the model. CCSM3 has a fairly regular, large amplitude oscillation with a period of about 20 years, although its amplitude decreases after 500 years, whereas CCSM4 shows much smaller variability with no regular oscillation. This change is mostly caused by the implementation of a new overflow parameterization in CCSM4, which is described in Danabasoglu et al. (2010). This parameterization improves the representation of the Denmark Strait and Greenland/Iceland/Scotland overflows, which results in North Atlantic Deep Water reaching down to 4km near 60°N, and is therefore more realistic. This highlights the fact that the representation of the North Atlantic MOC in the ocean components of climate models is rather sensitive to several of the parameterizations used. This

257



258

259

Figure 7. Time series of the maximum value in Sv of the North Atlantic meridional overturning circulation from the pre industrial control runs of the CCSM3 and CCSM4. From Danabasoglu et al. (2012).

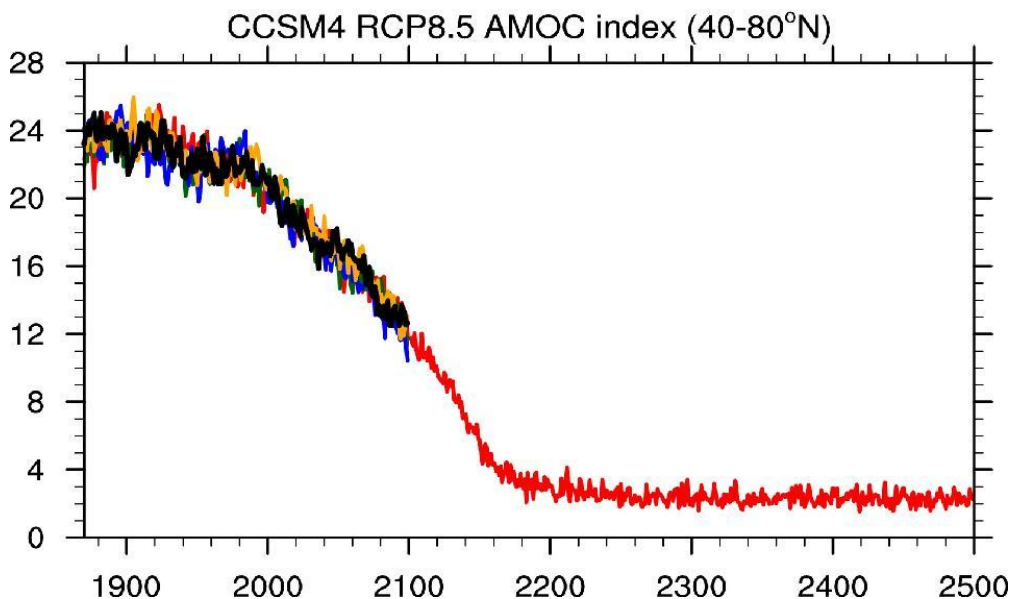
260

261 results in both the mean maximum value and the internal variability being quite different across all the climate  
262 models used to make future climate projections. Much more discussion of the North Atlantic MOC is in Chapter 5.6.

263 It has long been thought that future climate change could reduce the magnitude of the North Atlantic MOC,  
264 (Manabe et al., 1991). Both heating of the upper ocean and an increase in surface fresh water from melting sea ice  
265 and land ice, especially around Greenland, would reduce the density of the near surface water. This would increase  
266 the stability of the upper ocean compared to the deeper ocean, and hence has the potential to reduce the rate of deep  
267 water formation in the high latitude North Atlantic. There has also been much speculation that, if the MOC does  
268 reduce significantly, then Europe's climate could become colder in the future, rather than becoming warmer. The  
269 IPCC 4<sup>th</sup> Assessment Report covered the most recent work on this subject in Chapter 10.3.4 of Solomon et al.  
270 (2007). The results show that the MOC does get weaker in the future in all 19 climate models assessed, and the rate  
271 of weakening increases as the future rate of CO<sub>2</sub> rise increases in the forcing scenarios used. In addition, there is a  
272 range of weakening rates in the MOC across climate models that are forced with the same scenario CO<sub>2</sub> increase.  
273 The range of MOC decreases are bounded by no change at all in the commitment run where the CO<sub>2</sub> remains  
274 constant at the present day value, and a decrease of about 50% in the most sensitive models using a scenario where  
275 the CO<sub>2</sub> concentration has doubled from its 2000 value by the end of the 21<sup>st</sup> century. Some of these future  
276 projections have been run beyond 2100, where the CO<sub>2</sub> concentration is then kept constant at the 2100 value. In all  
277 'modern' models, and for all the scenarios used for CO<sub>2</sub> concentration at 2100, the MOC begins to strengthen once  
278 the CO<sub>2</sub> concentration is kept constant (Meehl et al. 2006, Solomon et al. 2007). Again, the rate of recovery  
279 depends on the particular model and the future scenarios used. 'Modern' here means full climate models using a  
280 horizontal resolution of 1° or finer, no flux adjustments, and modern physics in the ocean component including the  
281 much more physically realistic diffusion of heat and salt along sloping isopycnal surfaces rather than along  
282 horizontal surfaces. In addition, for all climate models and all future CO<sub>2</sub> scenarios used in the IPCC 4<sup>th</sup> Assessment  
283 Report, the radiative warming effect of the increased greenhouse gases over Europe is larger than the cooling effect  
284 of a reduction in the MOC. So, current climate models do not support a future cooling of Europe's climate,  
285 (Solomon et al. 2007).

286 It has frequently been suggested that the North Atlantic MOC could 'collapse' as a result of future increases in  
287 CO<sub>2</sub> concentration, and then remain at a very small magnitude for a long time into the future. Manabe and Stouffer  
288 (1993) showed that when the CO<sub>2</sub> concentration was quadrupled after 140 years and then held constant, the North  
289 Atlantic MOC did become very small, and then stayed very small for the duration of the 500 year integration.  
290 However, a later paper (Stouffer and Manabe 2003) shows that the MOC did recover after about 1500 years, and  
291 then stayed near to its initial value before CO<sub>2</sub> was increased for the remainder of the 5000 year run. The reason was  
292 that the warming near the surface diffused down slowly over the 1500 years, so that the upper 2-3 km of ocean  
293 became less stratified, and deep water formation started again. Thus, the MOC recovery time was set by the  
294 diffusive timescale for heat to reach the ocean mid-depths. When the same run up to 4xCO<sub>2</sub> was made with more  
295 'modern' climate models, then the MOC did start to recover soon after the CO<sub>2</sub> was held constant in both the  
296 HadCM3 (Wood et al. 2003) and the CCSM3 (Bryan et al. 2006b). Therefore, I believe that the Manabe and  
297 Stouffer (1993) result is influenced by the very coarse ocean resolution of about 4° in the horizontal and 12 vertical  
298 levels, horizontal mixing of heat and salt, and the large flux adjustments of heat and fresh water. Mikolajewicz et al.  
299 (2007) also showed that the North Atlantic MOC can become small and stay small when the increase in CO<sub>2</sub> is a  
300 factor of 5, and sometimes when it is a factor of 3. However, the horizontal resolution of their model is very coarse  
301 at 5.6°, and it has a very large flux adjustment of fresh water in the North Atlantic. The question then arises: Is there  
302 a final CO<sub>2</sub> concentration where the MOC becomes very small and subsequently does not recover in 'modern'  
303 climate models? Very recently, the Representative Concentration Pathway 8.5 (RCP8.5) has been used to force the  
304 CCSM4 between 2005 and 2300 from the end of a 20<sup>th</sup> century run from 1850 to 2005. The CO<sub>2</sub> starts at 285 ppm  
305 in 1850, is 385 ppm in 2000, and rises to near 1962 ppm by 2250 before leveling off. This run has already been  
306 discussed in Chapter 1.1. The globally-averaged surface temperature and the North Atlantic MOC index from  
307 Meehl et al. (2012) are shown in Figure 1.1.13. The MOC index starts at ~25 Sv in 1850, reduces to ~8 Sv in 2250,  
308 and remains near this value as the CO<sub>2</sub> forcing becomes almost constant. The average surface temperature in the

309 Arctic Ocean has risen by more than 20° C by 2300 in this RCP8.5 run, and there is no sea ice in the Arctic all year  
 310 round. The deep water formation in the Labrador Sea, Greenland-Iceland-Norwegian Seas, and Arctic Ocean is  
 311 completely shut off by 2200 because of the large rise in SSTs and rapid freshening in surface salinity caused by the  
 312 sea ice melt. The maximum of the MOC streamfunction north of 40°N, shown in Figure 8, has fallen to ~3 Sv by  
 313 2200, so that the index of ~8 Sv shown in Figure 1.1.13 is associated with the subtropical gyre near 20°N at 500 m  
 314 depth, rather than the MOC itself. This run has been continued out to 2500 with constant CO<sub>2</sub> forcing, and the  
 315 maximum MOC value north of 40°N remains <3 Sv throughout to 2500. If this run were to be continued further, I  
 316 think that the MOC would remain small for several hundred years, and a recovery would probably be on the long  
 317 diffusive timescale of heat to reach the ocean mid-depths, as in the 5000 year run of Stouffer and Manabe (2003).  
 318 Thus, the CCSM4 does show that its MOC can be switched off quasi-permanently when it is forced by a CO<sub>2</sub> rise of  
 319 a factor of almost 7 between 1850 and 2250. I suspect that other ‘modern’ climate models display similar behavior  
 320 when the forcing is so strong that all the Arctic sea ice melts, and deep water formation completely shuts off.  
 321



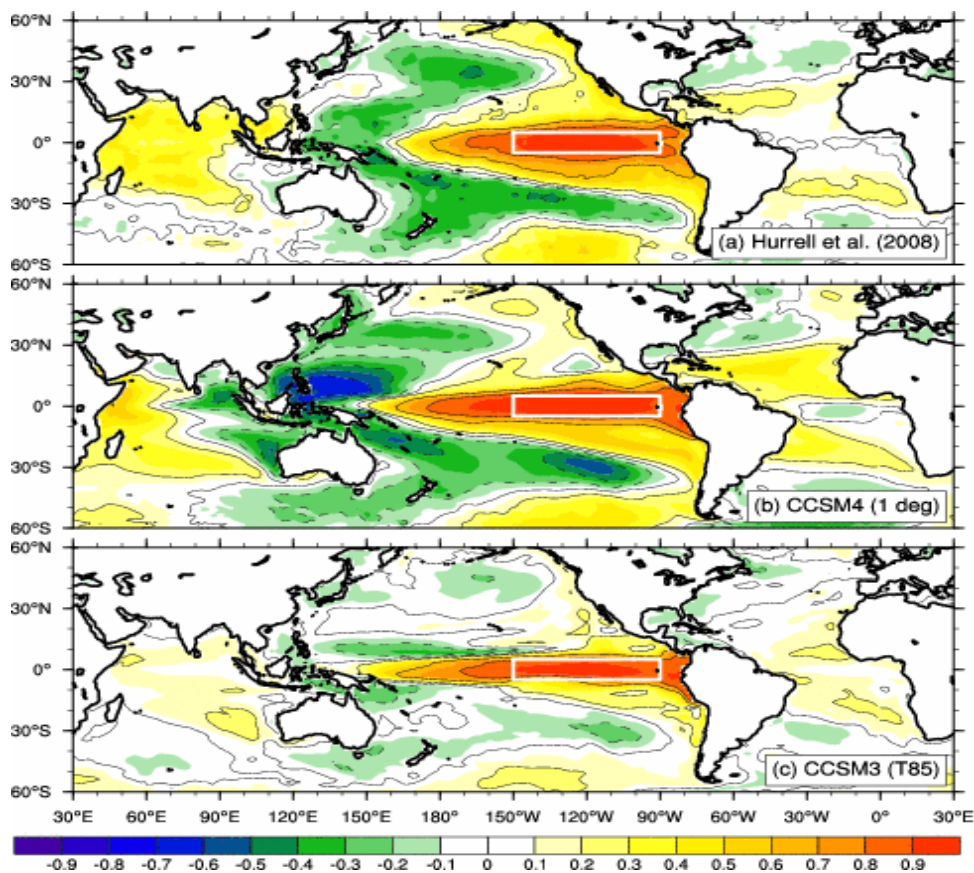
322  
 323  
 324 Figure 8. Maximum value of the North Atlantic MOC streamfunction north of 40°N in an ensemble of CCSM4  
 325 RCP8.5 runs, and in one extension from 2100 to 2500: The CO<sub>2</sub> value is constant after 2300. Courtesy of A. Hu.  
 326

327 Stommel (1961) showed that in a simple box model the MOC could possess multiple equilibria, which is two  
 328 different stable solutions with the MOC either strong or weak, given identical forcing of the model. In addition,  
 329 Marotzke and Willebrand (1991), Hughes and Weaver (1994) and many more recent studies have found multiple  
 330 equilibria of the MOC in global ocean models that use very coarse resolution of about 4°, diffusion of heat and salt  
 331 along horizontal surfaces, and are forced by mixed boundary conditions of restoring to an atmospheric temperature,  
 332 but an imposed flux of fresh water. More recently, Marsh et al. (2004) and Sijp et al. (2012) have found MOC  
 333 multiple equilibria in Intermediate Complexity coupled models that use a full ocean component with coarse  
 334 resolution, but a considerably simplified atmosphere component. The last of these results is despite the fact that,  
 335 using the same model, Sijp et al. (2006) find that the stability of North Atlantic deep water formation to imposed  
 336 fresh water inputs is significantly increased when diffusion of heat and salt along horizontal surfaces is replaced by  
 337 diffusion along sloping isopycnal surfaces. The reason is that vertical exchange can then be accomplished by the  
 338 diffusion, whereas it has to be accomplished by convection when the diffusion is along horizontal surfaces. Manabe  
 339 and Stouffer (1988, 1999) did find multiple equilibria of the North Atlantic MOC in a full climate model. However,  
 340 I believe this result is a consequence of the very coarse ocean resolution, horizontal mixing of heat and salt, and the  
 341 very large flux adjustment of fresh water. I know of no evidence of multiple equilibria of the North Atlantic MOC in

342 full, 'modern' climate models, so there are two possible explanations. Either multiple equilibria of the MOC exist in  
343 full climate models, but have not yet been found because of computational time constraints, or they do not exist  
344 when all the ocean-atmosphere feedbacks are working, which is not the case in Intermediate Complexity climate  
345 models. I favor the second explanation, but am willing to be proved wrong.

#### 346 5.4.7. El Nino/Southern Oscillation

347 ENSO is the largest and best observed interannual signal in the Earth's climate system. However, it has proved  
348 rather difficult to simulate well in climate models. Most models have difficulty reproducing the mean precipitation  
349 pattern in the tropical Pacific Ocean, because they have too much rain south of the equator in the western ocean that  
350 reaches too far into the central Pacific. In addition, the frequency of model ENSO variability in several models is  
351 too short, and is not the broad-band maximum between 3 and 7 years seen in observations. Much work over recent  
352 years has resulted in good ENSO simulations in a small number of climate models, such as the Hadley Centre  
353 HadCM3 (Collins et al., 2001), the GFDL CM2.1 (Wittenberg, 2009), and the CCSM4 (Deser et al., 2012). These  
354 improvements have resulted mainly from refinements to the deep convection parameterizations in the atmosphere  
355 components of these models, and from increased resolution in both the atmosphere and ocean; Guilyardi et al.  
356 (2009). Figure 9 shows the correlation of monthly mean NINO3 SST anomalies with global SST anomalies from  
357 observations, and the CCSM versions 3 and 4. The improvements in the CCSM4 are the much wider region of  
358 positive correlation in the eastern Pacific Ocean that reaches into the subtropics, and the horseshoe pattern of  
359



360

361 Figure 9. Correlation of monthly mean NINO3 (defined by the white box) SST anomalies with global SST anomalies from:  
362 a) Observations, b) the CCSM version 4, and c) the CCSM version 3. From Gent et al. (2011).

363 negative correlation in the west Pacific Ocean that extends into the central Pacific Ocean at mid-latitudes.  
364 Degrations are that the negative correlation is now much stronger than observations in the western Pacific Ocean,  
365 and it reaches into the east tropical Indian Ocean, probably because the ENSO amplitude is too large. These  
366 improvements result from changes to the atmosphere component deep convection scheme; see Neale et al., (2008).

367 The models that now simulate ENSO well show large very low-frequency variability in its amplitude on decadal  
368 and centennial timescales. Wittenberg (2009) shows the Nino3 SST anomaly from a 2000 year control run using  
369 1860 conditions from the GFDL CM2.1 model, see Figure 1. The very low-frequency variability is large, and is  
370 reminiscent of the ENSO simulations from the earlier, much simpler coupled model of Zebiak & Cane (1987). A  
371 frequently asked question is how ENSO will change in the future. However, Wittenberg (2009) and Stevenson et al.  
372 (2012) show that the very low-frequency ENSO variability in the CM2.1 and CCSM4 control runs is so large, that  
373 runs of at least 500 years would be required in order to detect a statistically significant change. Therefore, these  
374 models suggest that ENSO variability in the 21<sup>st</sup> century will be large, but will not be statistically different than the  
375 intrinsic variability of ENSO if the climate were stationary and in equilibrium. Much more discussion of ENSO and  
376 its prediction is in Chapter 5.5.

#### 377 *5.4.8. Uses of Climate Models*

378 Sections 5.4.3 through 5.4.5 describe the use of climate models to simulate a control run when the forcing is  
379 stationary, the earth's climate from 1850 to the present time, and to make future climate projections out to 2100 and  
380 beyond. In addition to the variables and phenomena described above, these runs make future projections of the sea  
381 level rise due to the warming of the oceans and the regional changes in sea level due to changes in ocean circulation.  
382 There are two other factors that change sea level; the first is the sea level rise due to melting of ice on land,  
383 including mountain glaciers and the Greenland and Antarctic ice sheets (see Chapter 6.1). There is strong evidence  
384 from GRACE satellite data of increasing ice melt off Greenland, Antarctica and other land glaciers over the last  
385 decade (Velicogna, 2009, Rignot et al., 2011), and during this time it is estimated that this fresh water source has  
386 contributed an equal amount to sea level rise as the thermosteric rise due to warming of the oceans. This  
387 contribution to sea level rise can be included in a climate model, if it has components that represent land glaciers and  
388 the two large ice caps. Several climate models are now in the process of including these two components. The final  
389 contributor to sea level changes is the height of the earth's crust, which is affected by melting of the Greenland ice  
390 sheet, changes in the Earth's geoid, and glacial isostatic adjustment (Douglas et al., 2001). It is very unlikely these  
391 effects will be included in climate models, but they can be estimated using glacial rebound models (Kopp et al.,  
392 2010).

393 If a climate model has an interactive carbon cycle, then it must have a biogeochemistry module in its ocean  
394 component. Several climate models now do have an interactive carbon cycle, which means they predict the  
395 concentration of CO<sub>2</sub> in the atmosphere given a scenario of emissions, rather than taking the atmospheric  
396 concentration as an input. In this case, the model will make future projections of the oceanic carbon cycle, which  
397 can be used as a projection for future ocean acidification, and for how this affects the future state of marine  
398 ecosystems (see Chapters 6.4 and 6.5).

399 Another very important use of the control and 20<sup>th</sup> century climate model runs is to explore the mechanisms and  
400 processes of climate variability on all time scales. For time scales from the diurnal, through the seasonal cycle and  
401 out to the several year time scale of ENSO, the model mechanisms can be compared to our knowledge from ocean  
402 observations. However, ocean variability on decadal and longer time scales is not well documented by observations,  
403 so our knowledge of the mechanisms driving ocean decadal variability comes mostly from models. Another use of  
404 climate models is to document how ocean variability, such as the North Atlantic MOC described in Section 5.4.6,  
405 affects the atmosphere and sea ice. In general, climate models are used to assess how processes in one component  
406 affect all the other components of the climate system, which cannot be determined by runs of the individual  
407 components alone.

408 Another use of climate models is to run simulations for many different paleo-climates of the past. These range  
409 from the last glacial maximum 21,000 years ago when the orbital parameters were different (e.g. Otto-Bliesner et al.,

410 2006), to deep time experiments many million years ago, when the locations of the continents were very different  
411 (e.g. Kiehl & Shields, 2005).

412 Over the past 10 years or more, climate models have been used to make ENSO and seasonal forecasts out to six  
413 months or a year. The difference between a forecast and a future projection is that the climate system needs to be  
414 initialized to the current climate state in order to make a forecast, whereas it is not initialized to observations when  
415 making a projection. Making a seasonal forecast is similar to making a weather forecast for the next few days,  
416 except that in the climate system on seasonal time scales it is just as important to initialize the upper ocean state as  
417 well as the atmospheric state. For an ENSO forecast, it is only important to initialize the upper part of the tropical  
418 Pacific Ocean (Rosati et al., 1997), and seasonal forecasts require the upper ocean to be initialized globally. More  
419 information on these ENSO and seasonal forecasts is in Chapter 5.5. A very recent development is the use of  
420 climate models to make decadal forecasts of the future climate. For a decadal forecast, the deeper parts of all the  
421 oceans need to be initialized, not just the upper ocean, and it may also be important to initialize the current state of  
422 sea ice in the Arctic and Antarctic, and the levels of soil moisture in the land component, although this is as yet  
423 unproven. Initializing the full depth ocean component is a major new challenge because it is a new aspect of ocean  
424 science, and much more information and details of decadal forecasts are in Chapter 5.6.

425 Obtaining an estimate of the current ocean state entails assimilating ocean data into a run of an ocean model that  
426 is driven by the best estimate of atmosphere forcing over the past few years. This has been done much more  
427 frequently with atmosphere models to produce 'reanalyses' of the past state of the atmosphere. It is now done  
428 routinely by several groups using ocean models, and some ocean 'reanalyses' have been produced recently (see  
429 Chapter 5.3). The accuracy of these 'reanalyses' has increased over the past few years (Carton & Santorelli, 2008),  
430 not only because of the experience obtained, but mostly because since about 2003 there are many more observations  
431 of temperature and salinity down to 2 km depth that have been obtained using ARGO floats (Roemmich et al.,  
432 2009). However, whether these 'reanalyses' are accurate enough to initialize the ocean component so that climate  
433 models can make useful decadal forecasts is a research question still to be explored in the future.

#### 434 *5.4.9. Limitations of Climate Models*

435 The standard future projections of climate change made with the current models mostly use a horizontal  
436 resolution of around  $1^\circ$  or a little finer in all the components, and quite coarse resolution in the vertical. Almost  
437 certainly, the largest limitation of  $1^\circ$  resolution is that several very important processes must be parameterized  
438 because they cannot be resolved. Probably the best known of these processes is clouds in the atmosphere  
439 component. It has been known since the first climate models were assembled that the radiative properties, including  
440 the greenhouse effect, depend strongly on the various cloud parameterizations that have been used in different  
441 models (Cess et al., 1989). The various cloud schemes, and the parameterization of the interaction between aerosols  
442 and clouds, also dictate to a large degree the model equilibrium climate sensitivity, which is the globally averaged  
443 surface temperature increase in response to a doubling of the carbon dioxide concentration. Despite almost thirty  
444 years of research, the range of model equilibrium climate sensitivities remains about a factor of two.

445 In the ocean component, a resolution of  $1^\circ$  means that the viscosity required has to be much higher than desired  
446 or used in higher resolution models, so that the intrinsic variability is much smaller than in the real ocean. Also, a  
447 resolution of  $1^\circ$  only begins to resolve the first Rossby radius of deformation near the equator, which is helped by  
448 the finer meridional resolution which is often used around the equator. Therefore, the effects of mesoscale eddies  
449 have to be parameterized. Most climate models use the Gent & McWilliams (1990) (GM) eddy parameterization,  
450 but there are significant differences in how it is implemented near the ocean surface, in the value of the coefficient  
451 chosen, and whether the coefficient is a constant or varies with position. It has been shown that a resolution of  $1/10^\circ$   
452 is necessary to resolve the eddy effects so that a model's sea surface height variability matches that from satellite  
453 observations (Bryan et al., 2006a). Thus, it will still be over a decade before eddy-resolving ocean components will  
454 be used for standard climate projections. However, some climate model control runs with the ocean and sea ice  
455 components using  $1/10^\circ$  resolution have recently been completed, (McClean et al. 2011, Kirtman et al. 2012). In  
456 general, these high resolution integrations have a worse climate in many respects compared to the coarse resolution

457 runs because we have less experience in how to choose the best parameter values. Chapter 3.4 shows how these  
458 high resolution integrations can be used to evaluate the GM parameterization.

459 Another important limitation of climate models is that they lack components that may be important for simulating  
460 certain potentially large future changes in the climate system. Good examples have already been mentioned, such as  
461 an active carbon cycle and a component for the Greenland and Antarctic ice sheets. Without these components, a  
462 climate model cannot address the possibility that the ocean will take up a smaller fraction of the CO<sub>2</sub> output in the  
463 future, which will leave a larger fraction in the atmosphere, and the future sea level rise due to water melting from  
464 the ice sheets. In addition, there are several more possibilities of severe, possibly abrupt, climate changes with a  
465 very small probability, but with very large consequences. Examples are the release of large amounts of methane  
466 from ocean clathrates (Archer, 2007) and the possible fast breakup of the West Antarctic Ice Sheet (Bamber et al.,  
467 2009). These are difficult to simulate accurately and to assess quantitatively the possibilities that they will occur.

#### 468 *5.4.10. Cutting Edge Issues*

469 The numerical discretization of the depth coordinate ocean components that are used in most climate models are  
470 quite old. They are based on latitude and longitude grids, although nearly all models now transpose the North Pole  
471 into a nearby land mass. There are also grids that have two poles in northern land masses, so that the resolution of  
472 the Arctic Ocean can be more comparable to the resolution in the rest of the global oceans. However, over the past  
473 ten years there has been much work on new grids that are much more uniform over the globe than latitude and  
474 longitude grids. These have mostly been developed with the atmosphere component in mind, and have been  
475 designed to work efficiently on the tens of thousands of processors that make up modern supercomputers (Staniforth  
476 & Thuburn, 2012). These grids can be made to vary in resolution from one part of the globe to another quite  
477 routinely. Therefore, the prospect is that grids with variable resolution will soon be available for global ocean  
478 components. Where to enhance the resolution and where to keep it coarse will then have to be decided, but  
479 enhanced resolution at the equator, along coasts and to resolve important narrow passages is now in prospect. The  
480 hope is that a variable grid would have many fewer grid points than a global 1/10° resolution grid, but would give  
481 comparable results.

482 Also over the past ten years, it has been well documented that depth coordinate models contain some cross-  
483 isopycnal mixing due to the numerics (Griffies et al., 2000, Ilicak et al., 2012). This is a problem if the numerical  
484 mixing is comparable to the very small level of cross-isopycnal mixing imposed in the deeper ocean. One way to  
485 avoid this is to use an isopycnal model where the vertical coordinate is potential density (Bleck, 2002, Hallberg,  
486 2000). This type of model can be run stably with no cross-isopycnal mixing at all. Some climate models use an  
487 isopycnal ocean component (Furevik et al., 2003, Sun & Bleck, 2006, Dunne et al., 2012), but still the large majority  
488 of climate models use a depth coordinate ocean component. One reason is familiarity, but benefits of depth  
489 coordinates are the ease of simulating the upper mixed layer and that they keep uniform vertical resolution  
490 throughout the global ocean. Maintaining realistic deep overflows has also been a traditional problem using depth  
491 coordinates, but this can be improved by incorporating an explicit overflow parameterization (Danabasoglu et al.,  
492 2010). Isopycnal coordinate models represent deep overflows quite well, but their traditional drawbacks are the  
493 difficulty of representing the mixed layer, where vertical density gradients are small, and poor resolution in the high-  
494 latitude oceans, where the top-to-bottom density gradient is very small. I think that both types of models should  
495 continue to be developed, so that the positives and negatives of the two coordinate systems can be further compared  
496 and contrasted. A third vertical coordinate system used in coastal ocean models is sigma, or terrain-following,  
497 coordinates, which automatically have very thin grid cells in the shallow regions of the ocean. This is an advantage  
498 when studying coastal currents and processes, but is a real disadvantage in the climate context. The reason is that  
499 the allowable time step due to vertical advection in the shallow ocean is much smaller than that using the other  
500 vertical coordinates, so that the ocean model takes much more computer time to run.

501 As important as upgrading the numerical aspects of ocean climate components is further development of all the  
502 parameterizations used in the model. The vertical mixing scheme in the momentum and tracer equations not only  
503 sets the mixed layer and thermocline depths, but also dictates the amount of cross-isopycnal mixing in the deeper

504 ocean. It should include contributions from many sources such as internal wave breaking, tidal mixing, possibly  
505 mesoscale eddies and other processes (see Chapter 3.3). It also needs to work well across a range of vertical  
506 resolutions, because the vertical grid varies considerably with depth in most models. How to specify the coefficient  
507 in the GM eddy parameterization as a function of position is the subject of ongoing work (Eden et al., 2009), as well  
508 as how to transition the GM scheme into horizontal tracer mixing in the mixed layer (Danabasoglu et al., 2008,  
509 Ferrari et al. 2010), (see Chapter 3.4). The prospect of variable resolution grids discussed above leads to the  
510 requirement that ocean component parameterizations work well over a large range of scales. A good example is the  
511 GM parameterization for the effects of eddies on the mean flow. How should the coefficient be specified in a grid  
512 that varies between  $1^\circ$  and  $1/10^\circ$ ? The same question needs to be asked of the horizontal viscosity scheme.

513 A final cutting edge issue is which processes and interactions are missing from current ocean components that  
514 could be important in future climate change? One example is the interaction of the ocean with ice shelves. This is  
515 very important because the breakup of small ice shelves has already been observed in Greenland and the Antarctic  
516 Peninsula. There is some potential for much larger Antarctic ice shelves to break up into the ocean. Current ocean  
517 components do not include the coastal and estuarine environments. These are areas of strong interactions between  
518 physical ocean properties and the carbon cycle. It is also where nutrients are injected from river outflows and most  
519 ocean biology occurs. These are potentially important aspects of the climate system, which are discussed in  
520 Chapters 6.3, 6.4 and 6.5.

521

522

## 523 Acknowledgments

524

525 I would like to thank my NCAR colleagues: Gokhan Danabasoglu for Figures 6 and 7, Marika Holland for Figure 3,  
526 Jerry Meehl for Figure 5, and Rich Neale for Figure 9. Aixue Hu ran the continuation of the CCSM4 RCP8.5 run  
527 out to 2500, and provided Figure 8. Thanks is also due to several colleagues at GFDL: Andrew Wittenberg for  
528 Figure 1, and Tom Knutson for Figures 2 and 4. Steve Griffies, Ron Stouffer, and two other reviewers provided  
529 very thorough reviews of this chapter, which contributed to a much improved final version. Thomas Stocker  
530 provided some comments, and his views on AMOC bifurcations and the possibility of multiple equilibria in full  
531 climate models.

532

533

## 534 References

535 Archer, D., (2007). Methane hydrate stability and anthropogenic climate change. *J. Geophys. Res.-Biogeo.*, 4, 521-  
536 544.

537 Bamber, G. L., R. E. Riva, B. L. Vermeersen, & A. M. LeBrocq, (2009). Reassessment of the potential sea-level  
538 rise from a collapse of the West Antarctic ice sheet. *Science*, 324, 901-903.

539 Bleck, R., (2002). An oceanic general circulation model framed in hybrid isopycnic-Cartesian coordinates. *Ocean*  
540 *Modelling*, 37, 55-88.

541 Boville, B. A. & P. R. Gent, (1998). The NCAR Climate System Model, version one. *J. Climate*, 11, 1115-1130.

542 Bryan, F.O., M.W. Hecht, & R.D. Smith, (2006a). Resolution convergence and sensitivity studies with North  
543 Atlantic circulation models. Part I: The western boundary current system. *Ocean Modelling*, 16, 141-159.

544 Bryan, F. O., G. Danabasoglu, N. Nakashiki, Y. Yoshida, D-H. Kim, J. Tsutsui, & S. C. Doney, (2006b). Response  
545 of the North Atlantic thermohaline circulation and ventilation to increasing carbon dioxide in CCSM3. *J.*  
546 *Climate*, 19, 2382-2397.

547 Bryan, K., S. Manabe, & R. C. Pacanowski, (1975). A global ocean-atmosphere climate model. Part II. The  
548 oceanic circulation. *J. Phys. Oceanogr.*, 5, 30-46.

549 Carton, J. A. & A. Santorelli, (2008). Global decadal upper-ocean heat content as viewed in nine analyses. *J.*  
550 *Climate*, 21, 6015-6035.

551 Cess, R. D., & Coauthors (1989). Interpretation of cloud-climate feedback as produced by 14 atmospheric general  
552 circulation models. *Science*, 245, 513-516.

553 Chassignet, E. P., L. T. Smith, R. Bleck, & F. O. Bryan, (1996). A model comparison: Numerical simulations of the  
554 north and equatorial Atlantic Oceanic circulation in depth and isopycnic coordinates. *J. Phys. Oceanogr.*, 26,  
555 1849–1867.

556 Collins, M., S. F. Tett, & C. Cooper, (2001). The internal climate variability of HadCM3, a version of the Hadley  
557 Centre coupled model without flux adjustments. *Clim. Dyn.*, 17, 61-81.

558 Cunningham, S. A. & Coauthors, (2007). Temporal variability of the Atlantic meridional overturning circulation at  
559 26.5° N. *Science*, 317, 935-938.

560 Danabasoglu, G., R. Ferrari, & J. C. McWilliams, (2008). Sensitivity of an ocean general circulation model to a  
561 parameterization of near-surface eddy fluxes. *J. Climate*, 21, 1192-1208.

562 Danabasoglu, G. & P. R. Gent, (2009). Equilibrium climate sensitivity: Is it accurate to use a slab ocean model? *J.*  
563 *Climate*, 22, 2494-2499.

564 Danabasoglu, G., W. G. Large, & B. P. Briegleb, (2010). Climate impacts of parameterized Nordic Sea overflows.  
565 *J. Geophys. Res.* 115, C11005, doi:10.1029/2010JC006243.

566 Danabasoglu, G., S. G. Yeager, Y. O. Kwon, J. J. Tribbia, A. S. Phillips, & J. W. Hurrell, (2012). Variability of the  
567 Atlantic meridional overturning circulation in CCSM4. *J. Climate*, 25, 5153–5172.

568 Deser, C., A. S. Phillips, R. A. Tomas, Y. Okumura, M. A. Alexander, A. Capotondi, J. D. Scott, Y. O. Kwon, &  
569 M. Ohba, (2012). ENSO and Pacific decadal variability in Community Climate System Model version 4. *J.*  
570 *Climate*, 25, 2622-2651.

571 Douglas, B. C., M. S. Kearney, & S. P. Leatherman, (2001). Sea level rise: History and consequences. International  
572 Geophysics Series 75, Academic Press.

573 Dunne, J. P. & Coauthors, (2012). GFDL's ESM2 global coupled climate-carbon Earth system model. Part I:  
574 Physical formulation and baseline simulation characteristics. *J. Climate*, 25, 6646-6665.

575 Eden, C., M. Jochum, & G. Danabasoglu, (2009). Effect of different closures for thickness diffusivity. *Ocean*  
576 *Modelling*, 26, 47-59.

577 Ferrari, R., S. M. Griffies, A. J. Nurser, & G. K. Vallis, (2010). A boundary-value problem for the parameterized  
578 mesoscale eddy transport. *Ocean Modelling*, 32, 143-156.

579 Furevik, T., M. Bentsen, H. Drange, I. K. Kindem, N. G. Kvamstø, & A. Sorteberg, (2003). Description and  
580 evaluation of the Bergen climate model: ARPEGE coupled with MICOM. *Clim. Dyn.*, 21, 27-51.

581 Gent, P. R. & J. C. McWilliams, (1990). Isopycnal mixing in ocean circulation models. *J. Phys. Oceanogr.*, 20,  
582 150-155.

583 Gent, P. R., (2011). The Gent-McWilliams parameterization: 20/20 hindsight. *Ocean Modelling*, 39, 2-9.

584 Gent, P. R. & Coauthors, (2011). The Community Climate Model version 4. *J. Climate*, 24, 4973-4991.

585 Gordon, C., C. Cooper, C. A. Senior, H. Banks, J. M. Gregory, T. C. Johns, J. F. Mitchell, & R. A. Wood, (2000).  
586 The simulation of SST, sea ice extents and ocean heat transports in a version of the Hadley Centre coupled model  
587 without flux adjustments. *Clim. Dyn.*, 16, 147-168.

588 Griffies, S. M., R. C. Pacanowski, & R. W. Hallberg, (2000). Spurious diapycnal mixing associated with advection  
589 in a z-coordinate ocean model. *Mon. Wea. Rev.*, 128, 538-564.

590 Griffies, S. M. & Coauthors (2011). The GFDL CM3 coupled climate model: Characteristics of the ocean and sea  
591 ice simulations. *J. Climate*, 24, 3520-3544.

592 Guilyardi, E. & Coauthors (2009). Understanding El Nino in ocean-atmosphere general circulation models:  
593 Progress and challenges. *Bull. Amer. Met. Soc.*, 90, 325-340.

594 Hallberg, R. W., (2000). Time integration of diapycnal diffusion and Richardson number-dependent mixing in  
595 isopycnal coordinate ocean models. *Mon. Wea. Rev.*, 128, 1402-1419.

596 Hirst, A. C., H. B. Gordon, & S. P. O'Farrell, (1996). Global warming in a coupled climate model including oceanic  
597 eddy-induced advection. *Geophys. Res. Lett.*, 23, 3361-3364.

598 Hughes, T. M. C. & A. J. Weaver, (1994). Multiple equilibria of an asymmetric two-basin ocean model. *J. Phys.*  
599 *Oceanogr.*, 24, 619-637.

600 Ilıcak, M., A. J. Adcroft, S. M. Griffies, & R. W. Hallberg. (2012). Spurious diapycnal mixing and the role of  
601 momentum closure. *Ocean Modelling*, 45, 37-58.

602 Kiehl, J. T. & C. A. Shields (2005). Climate simulation of the latest Permian: Implications for mass extinction.  
603 *Geology*, 33, 757-760.

604 Kirtman, B. P. & Coauthors, (2012). Impact of ocean model resolution on CCSM climate simulations. *Clim. Dyn.*,  
605 39, 1303-1328.

606 Kopp, R. E., J.X. Mitrovica, S.M. Griffies, J. Yin, C.C. Hay, & R.J. Stouffer, 2010: The impact of Greenland melt  
607 on local sea levels: a partially coupled analysis of dynamic and static equilibrium effects in idealized water-  
608 hosing experiments. *Climatic Change*, 103, 619-625.

609 Knutson, T. R., & Coauthors, (2006). Assessment of twentieth-century regional surface temperature trends using  
610 the GFDL CM2 coupled models. *J. Climate*, 19, 1624-1651.

611 Levitus, S., T. Boyer, M. Conkright, D. Johnson, T. O'Brien, J. Antonov, C. Stephens, & R. Gelfeld, (1998).  
612 *Introduction*, Vol. 1, *World Ocean Database 1998*, NOAA Atlas NESDIS 18.

613 Manabe, S., K. Bryan, & M. J. Spelman, (1975). A global ocean-atmosphere climate model. Part I. The atmospheric  
614 circulation. *J. Phys. Oceanogr.*, 5, 3-29.

615 Manabe, S. & R. J. Stouffer, (1988). Two stable equilibria of a coupled ocean-atmosphere model. *J. Climate*, 1,  
616 841-866.

617 Manabe, S., R. J. Stouffer, M. J. Spelman & K. Bryan, (1991). Transient responses of a coupled ocean-atmosphere  
618 model to gradual changes of atmospheric CO<sub>2</sub>. Part I: Annual mean response. *J. Climate*, 4, 785-818.

619 Manabe, S. & R. Stouffer, (1993). Century-scale effects of increased atmospheric CO<sub>2</sub> on the ocean-atmosphere  
620 system. *Nature*, 364, 215-218.

621 Manabe, S. & R. J. Stouffer, (1999). Are two modes of thermohaline circulation stable? *Tellus A*, 51, 400-411.

622 Marotzke, J. & J. Willebrand, (1991). Multiple equilibria of the global thermohaline circulation. *J. Phys.*  
623 *Oceanogr.*, 21, 1372-1385.

624 Marsh, R. & E. J. Coauthors (2004). Bistability of the thermohaline circulation identified through comprehensive 2-  
625 parameter sweeps of an efficient climate model. *Climate Dynamics*, 23, 761-777.

626 McClean, J. L. & Coauthors, (2011). A prototype two-decade fully-coupled fine-resolution CCSM simulation.  
627 *Ocean Modelling*, 39, 10-30.

628 Meehl, G. A. & Coauthors, (2006). Climate change projections for the twenty-first century and climate change  
629 commitment in the CCSM3. *J. Climate*, 19, 2597-2616.

630 Meehl, G. A. & Coauthors, (2012). Climate system response to external forcings and climate change projections in  
631 CCSM4. *J. Climate*, 25, 3661-3683.

632 Mikolajewicz, U., M. Groger, E. Maier-Reimer, G. Schurgers, M. Vizcaino & A. Winguth, (2007). Long-term  
633 effects of anthropogenic CO<sub>2</sub> emissions simulated with a complex earth system model. *Clim. Dyn.*, 28, 599-633.

634 Neale, R. B., J. H. Richter, & M. Jochum, (2008). The impact of convection on ENSO: From a delayed oscillator to  
635 a series of events. *J. Climate*, 21, 5904-5924.

636 Otto-Bliesner, B. L., E. C. Brady, G. Clauzet, R. Tomas, S. Levis, & Z. Kothavala, (2006). Last glacial maximum  
637 and holocene climate in CCSM3. *J. Climate*, 19, 2526-2544.

638 Randall, D. A., & Coauthors, (2007). Climate models and their evaluation. In *Climate Change 2007: The Physical  
639 Science Basis. Contribution of Working Group I to the fourth Assessment Report of the IPCC*. Cambridge  
640 University Press.

641 Rignot, E., I. Velicogna, M. R. Van den Broeke, A. Monaghan & J. Lenaerts, (2011). Acceleration of the  
642 contribution of the Greenland and Antarctic ice sheets to sea level rise. *Geophys. Res. Lett.*, 38, L05503,  
643 doi:10.1029/2011GL046583.

644 Roemmich, D., G. C. Johnson, S. Riser, R. Davis, J. Gilson, W. B. Owens, S. L. G. Owens, C. Schmid, & M.  
645 Ignaszewski, (2009). The Argo Program: Observing the global oceans with profiling floats. *Oceanography*, 22,  
646 24-33.

647 Rosati, A., K. Miyakoda, & R. Gudgel, (1997). The impact of ocean initial conditions on ENSO forecasting with a  
648 coupled model. *Mon. Wea. Rev.*, 125, 754-772.

649 Sausen, R., R. K. Barthels, & K. Hasselmann, (1988). Coupled ocean-atmosphere models with flux correction.  
650 *Clim. Dyn.*, 2, 154-163.

651 Sijp, W. P., M. Bates, & M. H. England, (2006). Can isopycnal mixing control the stability of the thermohaline  
652 circulation in ocean climate models? *J. Climate*, 19, 5637-5651.

653 Sijp, W. P., M. H. England & J. M. Gregory, (2012). Precise calculations of the existence of multiple AMOC  
654 equilibria in coupled climate models. Part I: Equilibrium states. *J. Climate*, 25, 282-298.

655 Solomon, S., D. Qin, M. Manning, Z. Chen, M. Marquis, K.B. Averyt, M. Tignor & H.L. Miller, (2007). *Climate  
656 Change 2007: The Physical Science Basis. Contribution of Working Group I to the Fourth Assessment Report of  
657 the IPCC*. Cambridge University Press.

658 Staniforth, A., & J. Thuburn, (2012). Horizontal grids for global weather and climate prediction models: a review.  
659 *Q. J. R. Meteorol. Soc.*, 138, 1-26.

660 Steele, M., R. Morley, & W. Ermold, (2001). PHC: A global ocean hydrography with a high-quality Arctic Ocean.  
661 *J. Climate*, 14, 2079-2087.

662 Stevenson, S., B. Fox-Kemper, M. Jochum, R. Neale, C. Deser, & G. Meehl, (2012). Will there be a significant  
663 change to El Nino in the 21st century? *J. Climate*, 25, 2129-2145.

664 Stommel, H., (1961). Thermohaline convection with two stable regimes of flow. *Tellus*, 13, 224-230.

665 Stouffer, R. J. & S. Manabe, (2003). Equilibrium response of thermohaline circulation to large changes in  
666 atmospheric CO<sub>2</sub> concentration. *Clim. Dyn.*, 20, 759-773.

667 Stouffer, R. J., (2004). Time scales of climate response. *J. Climate*, 17, 209-217.

668 Sun, S., & R. Bleck, 2006: Multi-century simulations with the coupled GISS-HYCOM climate model: Control  
669 experiments. *Clim. Dyn.*, 26, 407-428.

670 Velicogna, I., (2009). Increasing rates of ice mass loss from the Greenland and Antarctic ice sheets revealed by  
671 GRACE. *Geophys. Res. Lett.*, 36, L19503, doi:10.1029/2009GL040222.

672 Wittenberg, A. T., (2009). Are historical records sufficient to constrain ENSO simulations? *Geophys. Res. Lett.*, 36,  
673 L12702. doi:10.1029/2009GL038710.

674 Wood, R. A. & F. O. Bryan, (2001). Coupled ocean-atmosphere models. In *Ocean Circulation and Climate*, G.  
675 Siedler, J. Church, J. Gould Eds., International Geophysics Series 77, Academic Press.

676 Wood, R. A., M. Vellinga, & R. Thorpe, (2003). Global warming and thermohaline circulation stability. *Phil.*  
677 *Trans. R. Soc. Lond. A*, 361, 1961-1975.

678 Wunsch, C. & P. Heimbach, (2006). Estimated decadal changes in the North Atlantic meridional overturning  
679 circulation and heat flux 1993-2004. *J. Phys. Oceanogr.*, 36, 2012–2024.

680 Zebiak, S. E. & M. A. Cane, (1987). A model El-Nino-Southern Oscillation. *Mon. Wea. Rev.*, 115, 2262-2278.

681

682

## 683 Abstract

684 Coupled climate models consist of atmosphere, ocean, land and sea ice components. Most climate models now do  
685 not need to use flux adjustments to maintain the present day climate in a control run, when the forcings have a  
686 repeating annual cycle or are constant in time. A control run must simulate well known important large-scale  
687 phenomena, such as the El Nino/Southern Oscillation and the North Atlantic overturning circulation. Climate  
688 models are used to simulate the climate of the 20<sup>th</sup> Century, and to make projections of the future climate. The  
689 uses and limitations of climate models are then described, and several cutting edge issues are discussed.

690

## 691 Keywords

692 Coupled Models

693 North Atlantic overturning circulation

694 El Nino/Southern Oscillation

695 Control Runs

696 20<sup>th</sup> Century Runs

697 Future Climate Projections

698 Limitations of Climate Models

699 Cutting Edge Issues